Anal. Bioanal. Electrochem., Vol. 15, No. 8, 2023, 603-621
https://www.doi.org/10.22034/abec.2023.707322

Analytical & Bioanalytical Electrochemistry

Full Paper

Effect of Mn(II) Coordination Complexes on Corrosion Inhibition for Mild Steel in 1 M HCl Medium: Experimental, SEM-EDS Studies, DFT and MC Calculations

A. Radi,[1] A. Jmiai,[2] Y. Kerroum,[3] A. El-Asri,[2] M. Kaddouri,[1] M. El Massaoudi,[1] S. Radi,[1] B. El Ibrahimi,[2] B. El Mahi,[1] I. Warad,[4] A. Aouniti,[1] and A. Zarrouk[3]

[1]*Laboratory of Applied Chemistry & Environment, Faculty of Sciences, University Mohammed the First, MB 524, 60000 Oujda, Morocco*
[2]*Applied Physical Chemistry Laboratory, Faculty of Sciences, University of IBN ZOHR, B.P.8106 Dakhla District, Agadir, Morocco*
[3]*Laboratory of Materials, Nanotechnology, and Environment, Faculty of Sciences, Mohammed V University in Rabat, 4 Av. Ibn Battouta, B.P 1014 Rabat, Morocco*
[4]*Department of Chemistry, AN-Najah National University, P.O. Box 7, Nablus, Palestine*

*Corresponding Author, Tel.: +212665201397
E-Mail: azarrouk@gmail.com

Received: 9 April 2023 / Received in revised form: 31 July 2023 / Accepted: 16 August 2023 / Published online: 31 August 2023

Abstract- Materials decay naturally through a process called corrosion in which they react with their surroundings. It is possible to prevent mild steel from corroding in hydrochloric acid (HCl) by applying a variety of corrosion inhibitors. In this work, the novel mononuclear manganese coordination complex $[Mn(Hbpz)_2(NCS)_2]$ showed promising properties that make it suitable for corrosion prevention applications. In this experiment, different experimental methods were used to evaluate its inhibitory potential. For example, weight loss (WL) showed a 96% reduction in corrosion rate at higher concentrations. EIS was evidence that the concentration effect increases R_{ct} and reduces C_{dl}. Moreover, the polarization examination demonstrated that C3 is a mixed-type inhibitor. In addition, quantum mechanical and statistical methods were also used, and the effect of temperature was also determined. Besides, thermodynamic equations were used and calculated. The adsorption follows the Langmuir isothermal model and the simulation method confirmed the spontaneous adsorption nature of the complex, which improves the surface characterization results.

Keywords- Corrosion Inhibition; Mn(II) coordination complexes; EIS/PDP; SEM/EDS; DFT and MC simulation

1. INTRODUCTION

Corrosion of metals is a universally known phenomenon that causes every year material losses for the industry, it can lead to irreversible environmental degradation as well as loss of human lives; and health problems (pollution, contamination, ...) [1,2]. All these considerations justify an interest in corrosion control.

To combat corrosion, several methods have been developed, and one of the most practical methods is the use of organic inhibitors, the main characteristics of which are their ability to contain hetero-atoms that play a crucial role in improving the inhibitory properties of compounds, in particular, it works better in acidic environments such as hydrochloric acid (HCl) [3,4], and H_2SO_4 is occasionally referred to sulfur-containing compounds. Transition metal complexes have immense interest in coordination chemistry because of their applications in several fields. To evaluate the corrosion inhibition property of these compounds for mild steel in 1M HCl solution, experimental and theoretical studies were conducted. The changing of the counter anion changes the properties of the complexes [5]. Several research efforts are currently focused on the role of counter-anions in maintaining the arrangements of metal-organic complexes [6,7]. Various anions of different sizes and shapes forms such as Cl^- (spherical form) and NCS-(linear form) have been chosen and explored for the synthesis of NCS. In our experiment, when thiocyanate $[SCN]^-$ is introduced to a solution containing Fe^{3+} ions, $[Fe(NCS)(H_2O)_5]^{2+}$ is formed, turning the solution red [8]. The use of metal complexes as inhibitors in acidic solutions is very important to delay the corrosion of mild steel [9,10]. These complexes' biological activity is highly reliant on the way metal ions coordinate with one another and the binding sites on their ligands [11].

It is important to note that the proposal of this investigation is to provide complementary information on the inhibitory effect of $[Mn(Hbpz)_2(NCS)_2]$, using the polarization curves and the EIS can provide information on the mechanism of corrosion inhibition, while gravimetry offers a direct measurement of the rate of corrosion. And by combining SEM imaging with EDS analysis, we can provide valuable information about the microstructure, elemental composition, and surface topography of various mild steel surfaces. During this work, experimental results were compared to theoretical data.

2. EXPERIMENTAL METHODS

2.1. Organic synthesis

Organic synthesis of the molecule under test focuses on building organic compounds through chemical reactions. It involves the design and execution of various synthetic routes to obtain target molecules using a wide range of tools, equipment, and analytical instruments. The process of synthesizing molecules requires careful planning and consideration of reaction conditions, reagents, and purification methods to obtain the desired product. However, the steps

involved in the organic synthesis of the molecule may vary depending on the specific target molecule and the synthetic route desired, but the detailed steps can be found in these articles [12,13].

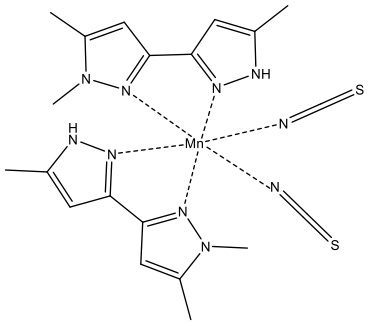

Scheme 1. The Synthetic mononuclear coordination complex $Mn(Hbpz)_2(NCS)_2$ (**C_3**)

2.2. Materials

The experimental work was carried out on mild steel (MS) generally comprising iron (Fe) as the main element with a carbon content of 0.21% and small amounts of manganese (0.05%), silicon (0.38%), Sulfur (0.05%), Aluminum (0.01%) and Phosphorus (0.09%). Sample preparation is guided as follows: Polishing with abrasive paper at different degrees from 180 to 1200, Rinse with distilled water to remove any debris or particles, Hot air drying [14].

2.3. Weight loss measurements

To determine the effect of compound inhibitor concentrations on the MS degradation process in 100 mL of 1 M HCl, the duration of 6 hours at a constant temperature of 308 K was tested and 2 cm × 2 cm × 0.25 cm dimensions square form steel samples were used. Inhibitory efficiencies were calculated following the Eq. (1) below:

$$E_W\,\% = \frac{W_0 - W_{corr}}{W_0} \times 100 \qquad (1)$$

which the corrosion rate reference is the degradation of MS in 1M HCl (**W_0**), and the effect of inhibitor concentrations is **W_{corr}**.

2.4. Electrochemical measurements

In this investigation, the electrochemical setup of a potentiostat (Voltalab PGZ 301) and Voltamaster 4 software were used as an experimental tool that made it possible to plot diagrams and curves of impedance and polarization, respectively. And in all electrochemical assays, we are utilized a double-walled cell with a thermometer. This cell is equipped with three electrodes: mild steel electrode as a working electrode to measure the current and potential of the reactions that occur on its surface when immersed in the solution, in the form of a circular

plate, palatine electrode called the auxiliary electrode completes the circuit, and saturated calomel electrode (SCE) serves to measure the potential of the working electrode.

These three kinds of electrodes were kept under atmospheric aeration conditions in all experiments for 30 minutes to control the electrochemical measurements of the working electrode [15]. For potentiodynamic polarization, the specific cases of a sweep speed constant (0.5 mV/s), and potential sweep range (-800 to -200 mV/SCE) were operated. Information about the resistance, capacitance, and other electrical properties of the working electrode was obtained by electrochemical impedance spectroscopy (EIS), the system involves the application of a small sinusoidal voltage with an amplitude of 10 mV, and the frequency range extends from 100 kHz to 10 mHz. The inhibitory efficiencies are estimated through equations (2) and (3):

$$E_{PDP}\% = \frac{i_{corr} - i_{corr(inh)}}{i_{corr}} \times 100 \quad (2)$$

$$E_{EIS}\% = \frac{R_{ct(inh)} - R_{ct}}{R_{ct(inh)}} \times 100 \quad (3)$$

where R_{ct} and i_{corr} are the transfer charge resistance and the corrosion current of the working electrode in 1 M HCl, respectively. $R_{ct(inh)}$ and $i_{corr(inh)}$ are the transfer charge resistance and the corrosion current of the working electrode in 1 M HCl plus inhibitor, respectively [16].

2.5. Surface characterization by SEM coupled to EDS

Scanning electron microscopy and energy-dispersive x-ray spectroscopy were focused to provide an investigation of the surface morphology and composition of the working electrode. The images are taken after 1 day of immersion in 1 M HCl in comparison with those taken in 1 M HCl plus inhibitor.

2.6. Quantum Chemical Calculations (DFT)

In order to describe reactivity, a number of descriptors have been extracted, dipole moment (μ), lowest unoccupied molecular orbital (LUMO), highest occupied molecular orbital (HOMO), and energy gap (ΔE gap). The software program Gaussian, module 9.0, was used to do quantum computations. A theoretical analysis of the chemicals under study using density functional theory DFT The CPCM solvation model was performed to treat the aqueous phase, with water as the solvent, utilizing the B3LYP hybrid functional level and the LanL2DZ basis set, which provides better results in terms of determining electronic and geometries properties.

2.7. Molecular dynamic (MD) simulations

The adsorption process of the C3 complex on the used metal surface was investigated using Monte Carlo simulations in the aqueous phase. To avoid possible inter supercellular

interactions which could be caused by the periodic boundary condition, the modelling was carried out in a simulation box of 20.34 Å × 20.34 Å × 50.26 Å in dimension [12], a vacuum layer sufficient thickness of 30 Å is achieved , the metal substrate was simulated by five surface layers of Fe(110) mild steel [17]. Electrostatic and Van der Waals interactions were treated using atomic summation and Ewald's methods. The UNIVERSAL is used as a force field [18,19]. The simulations were carried out using the Materials studio software (version 06).

3. RESULTS AND DISCUSSION

3.1. IR characterization

IR spectra are shown in Figure 1. The IR data for the Mn complex show the presence of peaks corresponding to the stretching/bending vibrations at 1623, 1635 and 1616 cm^{-1} respectively, were attributed to the stretching vibrational mode of the pyrazole ring. A downward shift of the bands from 18 to 37 in the complex indicates that the υ(C=N) group of the ligand is coordinated to the metal ion via its pyrazole nitrogen. in the IR spectra of the complex has been attributed to in-plane and out-of-plane βC-H bending vibrations, respectively. These vibrational bands appear at 1369(m) and 944(w), 786(w). The IR bands belonging to C-H bending, both asymmetric and symmetric were observed in the complexes within the range of 1491-1497 and 1271-1276 cm^{-1} respectively. Further the IR spectrum of complex of Mn showed the presence of anion NCS-. The splitting of the C≡N band at 2084 and 2064 cm^{-1} indicate the cis-configuration of the NCS ligand.

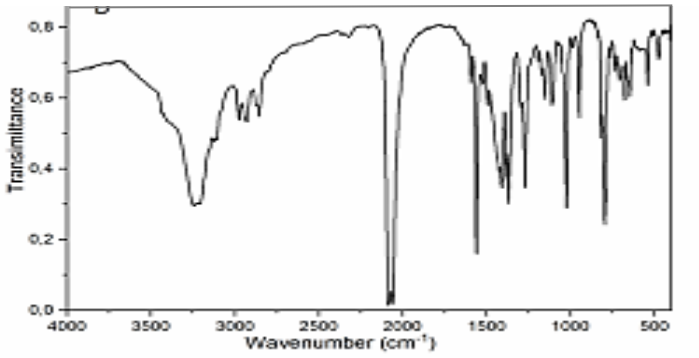

Figure 1. IR spectrum of complex of Mn

3.2. Weight loss study

The gravimetric analysis involves several steps, including sample preparation, immersion, washing, drying, and weighing. To provide more detail on the results, Table 1 summarizes the gravimetric test results for the C3 complex at different concentrations.

Table 1. Gravimetric measurements of different concentrations in the absence and presence of (C_3) in 1 M HCl

	C (M)	W (mg/cm²h)	IE (%)	Θ
Blank	1M	0.800	-	-
C3	10^{-6}	0.754	8.5	0.085
	10^{-5}	0.600	25.0	0.250
	10^{-4}	0.143	82.0	0.820
	10^{-3}	0.029	96.3	0.963

The study shows that the effectiveness of C3 as a corrosion inhibitor depends on its concentration, which resulted in a decrease in the corrosion rate of up to 96%, indicating that higher concentrations of C3 lead to better protection against corrosion. In addition, many authors discuss various types of organic inhibitors and provide insight into the mechanisms by which these inhibitors protect metals from corrosion. Moreover, this means that when the concentration of C3 increases, the protection it provides also increases. This relationship between inhibitor concentration and reduction in corrosion rate can be described by the fact that C3 constructs a defensive layer on the metal surface, preventing the corrosive environment from reaching it. This layer behaves as an impediment and reduces the rate of corrosion. The exploitation of organic corrosion inhibitors has been studied for several metals. They have been shown to be effective in acidic environments, which can significantly slow the rate of corrosion, and their effectiveness is concentration and temperature dependent.

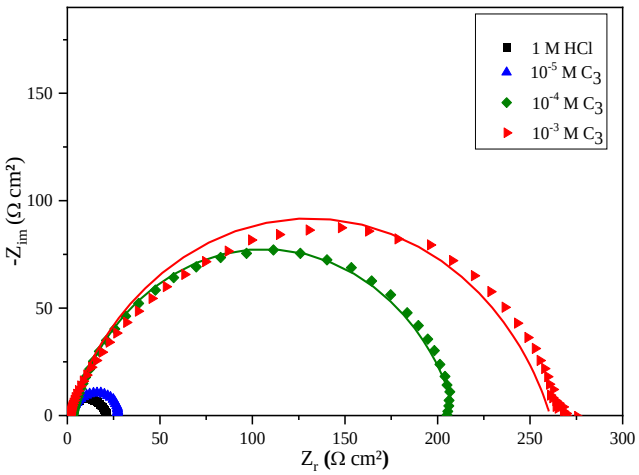

Figure 2. Concentrations effect of C3 complex on Nyquist plots of the metal

3.3. Electrochemical Impedance Spectroscopy (EIS)

EIS is an influential technique in the field of electrochemical measurements. It provides practical details about the electrical properties of electrochemical systems, including

electrodes, electrolytes, and interfaces [18,20]. The Nyquist diagram of steel at different concentrations of Manganese complex with NCS as an anion is displayed in (Figure 2). This diagram is obtained after 30 min of immersion at corrosion potential. We notice that the impedance plots show a capacitive loop. This pattern has a similar shape for all concentrations. Increasing inhibitor concentrations conduct to an increase in the size of the capacitive loop which leads to an enlargement in resistance to charge transfer.

Moreover, in this investigation, the equivalent electrical circuit that describes the different parameters is shown in the schematic (Figure 3) with (R_{ct}) charge transfer resistance, resistance to solutions (R_s) and C_{dl} is the double layer capacitance.

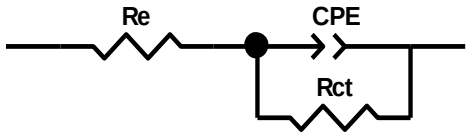

Figure 3. Modeling metal/solution using an electrical equivalent circuit

The capacity of double couch C_{dl} is calculated by the expression below:

$$C_{dl} = \frac{1}{2\pi f_{max} R_{ct}} \quad (4)$$

where f_{max} is the frequency at the top of the circle, the electrochemical parameters and inhibitory efficiencies are shown in the Table 2.

Table 2. Concentrations effect of C3 complex on metal electrical parameters

Medium	C (M)	R_e (Ω cm^2)	R_{ct} (Ω cm^2)	Q ($\mu\Omega^{-1}$ s^n cm^{-2})	n	C_{dl} (μF/cm^2)	E_{EIS} (%)
Blank	1	1.21±0.02	18.5±0.7	430.7±3.7	0.821±0.002	150.2	-
C3	10^{-5}	1.05±0.03	26.7±0.5	207.0±1.9	0.851±0.001	83.3	31
	10^{-4}	1.17±0.02	207.2±2.3	96.4±1.2	0.867±0.003	52.9	91
	10^{-3}	1.12±0.04	259.8±3.1	73.9±0.8	0.881±0.002	43.3	93

By analyzing the corrosion parameters of the system provided by impedance tests, valuable information about its electrochemical properties can be obtained. The results provided show that the inhibitor, when added to the studied system, affects two important EIS parameters: R_{ct} and C_{dl}, which the concentration effect augments R_{ct} and reduces C_{dl}. The fact that increases in R_{ct} suggests that the inhibitor impedes electron transfer at the electrode surface. This may be due to various reasons, such as the process by which the electrode surface retains the inhibitor molecules as a thin film or changes in local pH or redox potential caused by the inhibitor. The decrease in C_{dl} suggests that there is less charge storage capacity, which could also be due to inhibitor adsorption or other changes in surface chemistry [21].This appears in the effectiveness of the inhibitor which reaches 93% at the maximum concentration. Generally, a higher

concentration of inhibitor will lead to greater inhibition, of which the affinity of the inhibitor to the metal in question is an important factor in determining efficacy. High affinity inhibitors will bind tightly to the metal surface and be more effective in inhibiting its activity. Overall, understanding an inhibitor requires consideration of a number of factors that can influence its ability to inhibit a target metal or reaction.

3.4. Polarization studies

The polarization curves are processed to examine the behavior of the metal under the influence of the concentration of C3 complex in the medium of 1 M of hydrochloric acid. Specifically, they are used to measure the relationship between current density and applied potential while holding all other experimental parameters constant. The resulting curve can provide important information about the kinetics and thermodynamics of an electrochemical reaction. Figure 4 shows the Tafel plot of the substrate/inhibitor system at different concentrations, which provides important information about the electrochemical behavior of the system, relates the current density to the mechanism of the reaction, and gives a measure of the corrosion rate. It is also used to determine the corrosion potential of metal in a given environment. Electrochemical parameters and inhibitory efficiencies at different concentrations are shown in Table 3.

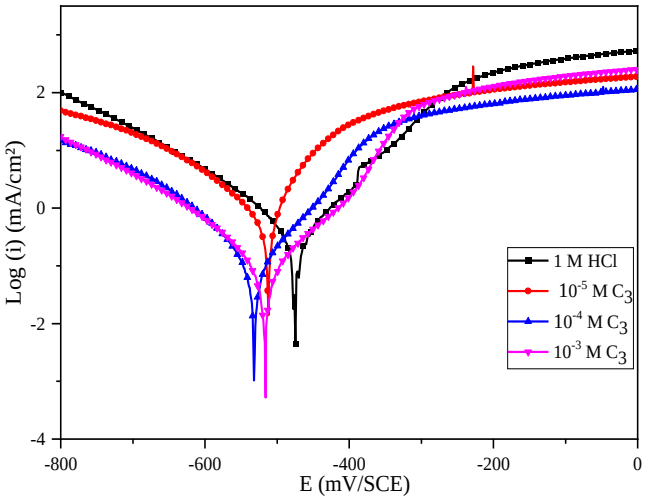

Figure 4. Concentrations effect of C3 complex on polarization curves of the metal

Table 3. Concentrations effect of C3 complex on metal corrosion parameters

Medium	Conc. (M)	$-E_{corr}$ (mV /SCE)	$-\beta_C$ (mV/dec)	β_a (mV/dec)	i_{corr} ($\mu A/cm^2$)	E_{PDP} (%)
Blank	1M	474.0	128	108	970.0	-
C3	10^{-3}	516.4	64.5	68.1	043.7	96
	10^{-4}	530.6	71.9	65.3	065.4	93
	10^{-5}	513.1	109.4	55.7	677.0	31

Corrosion current density is the rate at which corrosion occurs on a metal surface. It is a critical factor in estimating the effectiveness of inhibitors. Furthermore, Inhibitor concentration can greatly affect corrosion current density. In this substrate/inhibitor system, the added C3 complex diminishes the corrosion of the substrate material, and the Tafel plot of the system shows a decrease in both i_{corr} and β with increasing C3 complex concentration. This means that the C3 complex increases the activation energy of the reaction and as a consequence reduces the rate of corrosion, indicating an increase in efficiency with increasing concentration. The efficiency reaches an optimal value of 96% for the C3 complex at 10^{-3}M. Several studies have been conducted to explore the consequence of inhibitor concentration on the corrosion current density of substrate material in hydrochloric acid, which found that as the adsorption of the inhibitor increases, the corrosion current density drops to lower values [22,23]. In general, there is a correlation between inhibitor concentration and corrosion current density. Indeed, the inhibitor molecules are adsorbed on the surface of the metal and form a healing film that controls the corrosion process. The capacity of inhibition depends on characteristics such as the concentration, the properties of the metal, its surface quality, and the environment in which it is exposed.

3.5. Temperature effect and activation parameters and adsorption isotherm

In industry, many processes are performed at high temperatures. Therefore, in this research, the effect of temperature has been carefully studied using C3 compound. The results presented in Table 4 reveal that temperature plays an important role in the corrosion rate and effectiveness of the C3 complex, with higher temperatures accelerating the corrosion and reducing the efficiency, which may prove the desorption of C3 complex [24].

Table 4. Gravimetric data for temperature effect of C3

Medium	Temp. (K)	Conc. mol/L	Corrosion rate (mg/cm^2h)	E_W (%)
HCl	318	1	1.8251	-
	328	1	2.0564	-
	338	1	3.6500	-
	348	1	4.9721	-
C3	318	10^{-3}	0.1050	94
	328	10^{-3}	0.5180	75
	338	10^{-3}	1.2900	65
	348	10^{-3}	2.9700	40

To determine the activation energy (E_a), we plot the ln(W) curve as a function of 1/T (Figure 5) using the Arrhenius equation as follows [25]:

$$\ln W = -\frac{E_a}{RT} + \ln A \quad (5)$$

where W, A, T, and R are corrosion rate, pre-exponential constant, temperature and gas constant, respectively. We calculate the activation entropies (ΔS_a) and enthalpies (ΔH_a) using the relationship shown below:

$$\ln\frac{W}{T} = -\frac{\Delta H_a}{RT} + \frac{\Delta S_a}{R} + \ln\frac{R}{Nh} \quad (6)$$

N is Avogadro's number and h is Plank's constant respectively.

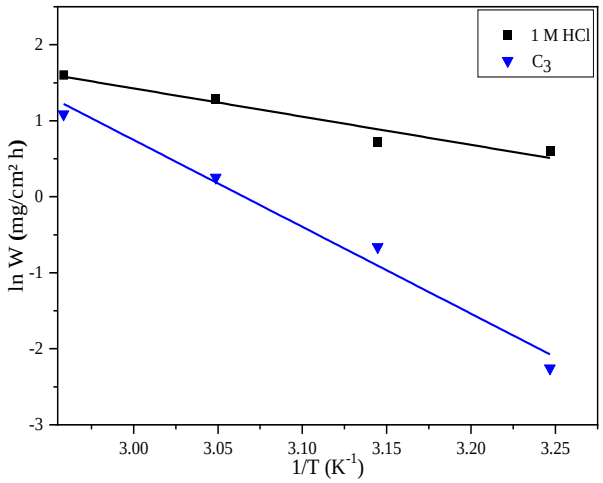

Figure 5. C3 complex effect on Arrhenius curves of the metal

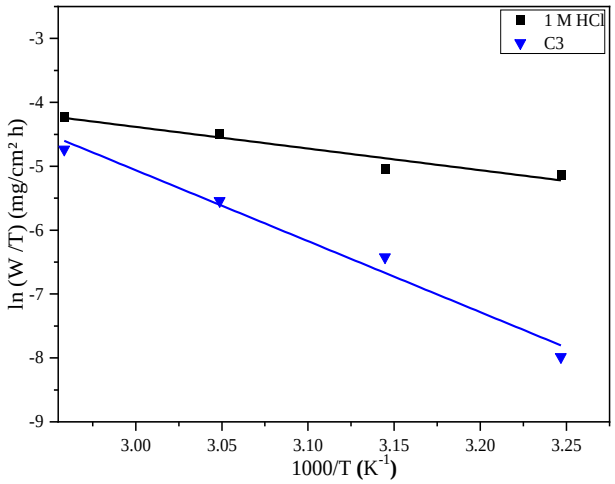

Figure 6. C3 complex effect on plot of ln(W /T) against (1000/T) of the metal

According to Figure 6 and Table 5, the minimum energy (E_a) required for a chemical reaction to occur in the case of the inhibited solution is higher than that of the uninhibited solution. This means that more energy is required to overcome the barrier created by the C3 complex. Besides, a positive value of ΔH_a indicates that heat must be supplied to start the reaction, and since it is increased by the C3 complex, it implies that more energy is required by the system to activate the corrosion process [27]. On another side, the value of entropy ΔS_a

is negative for uninhibited solution, and it is positive in the inhibited solution. Then it is an association step rather than a dissociation [28,29]. The value of ΔS_a explained by the disorder due to the large number of water molecules (the increase in solvent) desorbed from the surface by the C3 complex [30].

Table 5. C3 complex effect on the values of E_a, ΔH_a and ΔS_a for mild steel in in 1 M HCl

Medium	C	E_a (kJ mol^{-1})	ΔH_a (kJ mol^{-1})	ΔS_a (J mol^{-1}K^{-1})
HCl	1	32.82	30.05	-146.70
C3	10^{-3}	95.04	92.285	37.42

The equation below represents the Langmuir adsorption isotherm [26]:

$$\frac{C_{inh}}{\theta} = \frac{1}{K_{ads}} + C_{inh} \quad (7)$$

C_{inh} is the inhibitor concentration; θ is the surface covered fraction and K_{ads} is the equilibrium constant for the adsorption-desorption process.

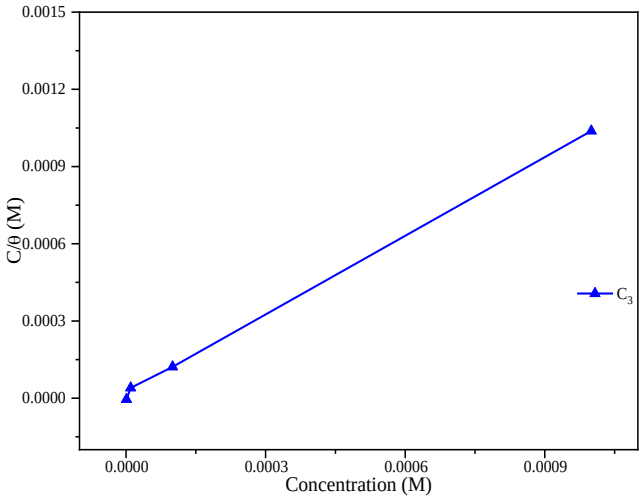

Figure 7. Langmuir adsorption plots of C3 complex on mild steel

To understand the phenomenon of adsorbate/substrate interface interactions, we study the adsorption isotherm (Figure 7), according to the obtained findings (Table 6) [31], we can conclude that the linear correlation coefficient and slope are close to unity for the C3 complex, we found that the Langmuir adsorption isotherm model is the most appropriate. The adsorption free energy is calculated according to the thermodynamic formula [32,33]:

$$\Delta G_{ads}^{0} = -RT \ln\left(55.5 K_{ads}\right) \quad (8)$$

The determinate values of ΔG^0_{ads} in this work (Table 6) show that the adsorption mechanism of the C3 inhibitor involves two types of interactions: Chemisorption and physisorption [34,35].

Table 6. Thermodynamic parameters of C3 complex/mild steel system

Compound	R^2	Slope	K (L mol^{-1})	ΔG^0_{ads} (kJ mol^{-1})
C3	0.9989	1.02	6.964 10^4	-38.84

3.6. Surface examination by SEM-EDS techniques

SEM and EDS techniques were performed to determine the elements present on the mild steel surface after 24-hour immersion in 1M hydrochloric acid with and without inhibitor C_3 (Figure 8a) with the sample that emerged in 1M HCl without inhibitor shows that the alloy surface is damaged.

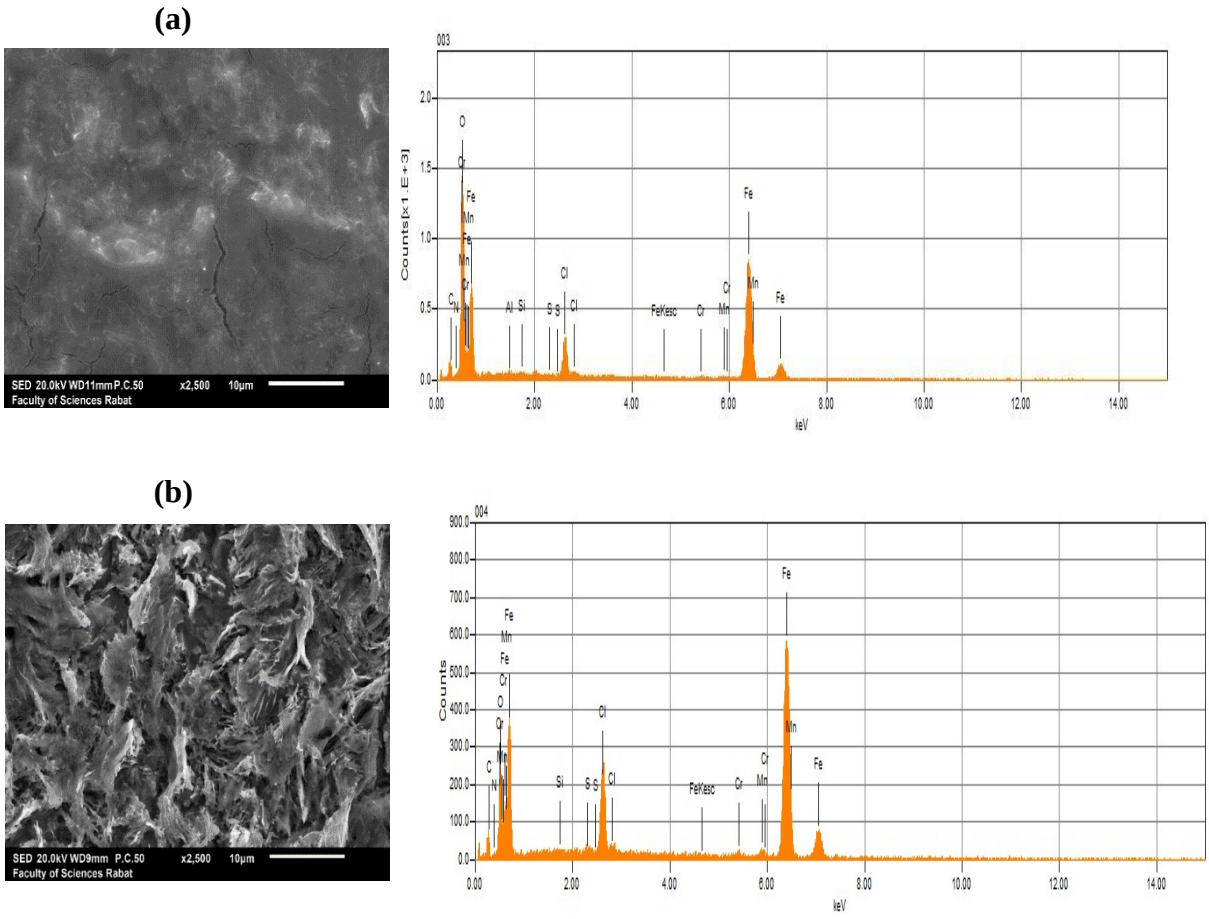

Figure 8. SEM image and EDS of the metal after immersion (a) 1 M HCl and (b) 10^{-3} M of C_3

Figure 8b, in the presence of $Mn(Hbpz)_2(NCS)_2$ complex, shows an improvement of the surface morphology which is covered by a protective film and thus a more homogeneous surface is formed due to the greater synergy. The appearance of the nitrogen and sulfur peak

of the thiocyanide anion NCS adsorbed on the surface enhances the stability of the complex. the interaction of the electron pair of the nitrogen and sulfur atom with the alloy surface, since the iron surface is positively charged in chloride acid medium [36,37].Our attention was focused on the formation of strong coordination bonds between the thiocyanate anion and the iron ion, the thiocyanate is an ambidextrous and bidentate ligand to bridge two metal atoms (M-SCN-M') and even tridentate (>SCN- or -SCN<)which implies the strong adsorption of the Mn complex (C3),which confirms the results obtained in the gravimetric studies.

3.7. Quantum chemical calculations

Along with improvements in computer technology and the development of effective algorithms, theoretical prediction of corrosion inhibitors' efficiency has recently gained a lot of popularity. These developments have facilitated the everyday development of molecular quantum mechanics computations [38,39]. In order to better understand the interactions between inhibitory compounds and metal surfaces, quantum chemical computations are used. The ability of inhibitor molecules to adsorb on the surface of a metallic material is inextricably tied to the molecular structures, energetics, and electronic properties of the compounds investigated. In this direction, Density Functional Theory (DFT) has been performed for quantum chemical calculations. Quantum parameters such as dipole moment (μ), energies (Total system $Energy_T$, E_{HOMO}, E_{LUMO} and ΔE), electronegativity (χ), global hardness (η), softness (σ) of the inhibitor and the fraction of electrons transferred from the inhibitor to the metal surface (ΔN) are grouped in Table 7.

We can see from the Table that the E_{HOM} energy of compound C3 was-4.571 eV; this is a more energetic value, which implies that this molecule can transfer electrons to the unoccupied d orbital of mild steel. While the E_{LUMO} energy (-1.252 eV "C3") was measured, which indicates that this molecule can take electrons from the metal. The Gap energy (ΔE) provides information on the reactivity of the molecule tested, according to Table 7we found that the ΔE of the tested complex (ΔE(C3) =3.318 eV) is a low energy; This indicates that the interactions between mild steel and the inhibitor are stronger. Some researchers have previously observed that increased inhibition efficiency is caused by higher values of dipole moment (μ) and smaller values of ΔE [38–40].We've established that the C3 complex have higher value of μ (25.126 Debye). This refers to the substance polarity assessed, which shows how easily the inhibitor interacts with the metal surface. According to the concept of electronegativity, hardness and softness for C3 molecule, we found positive values, indicating that this molecule had the largest electron accepting capability, facilitating its adsorption on the metal surface.

Furthermore, the fraction of transferred electrons (ΔN), which is an important measure for measuring the inhibition performance, shows the strength of the electron transfer. The positive value of ΔN and (ΔN<3.6) shows the spontaneity of electron transfer from the inhibitor

molecule (C3) to the unoccupied orbital of mild steel, which explains the improvement in inhibition efficiency [41,42].

Table 7. Quantum chemical parameters of tested inhibitor (C3) using DFT/B3LYP method with LANL2DZ basis set

	$Energy_T$ (ev)	E_{LUMO} (ev)	E_{HOMO} (ev)	ΔE (ev)	μ (Debye)	η	σ	χ	ΔN
C3	-37331.989	-1.252	-4.571	3.318	25.126	1.759	0.602	3.102	1.231

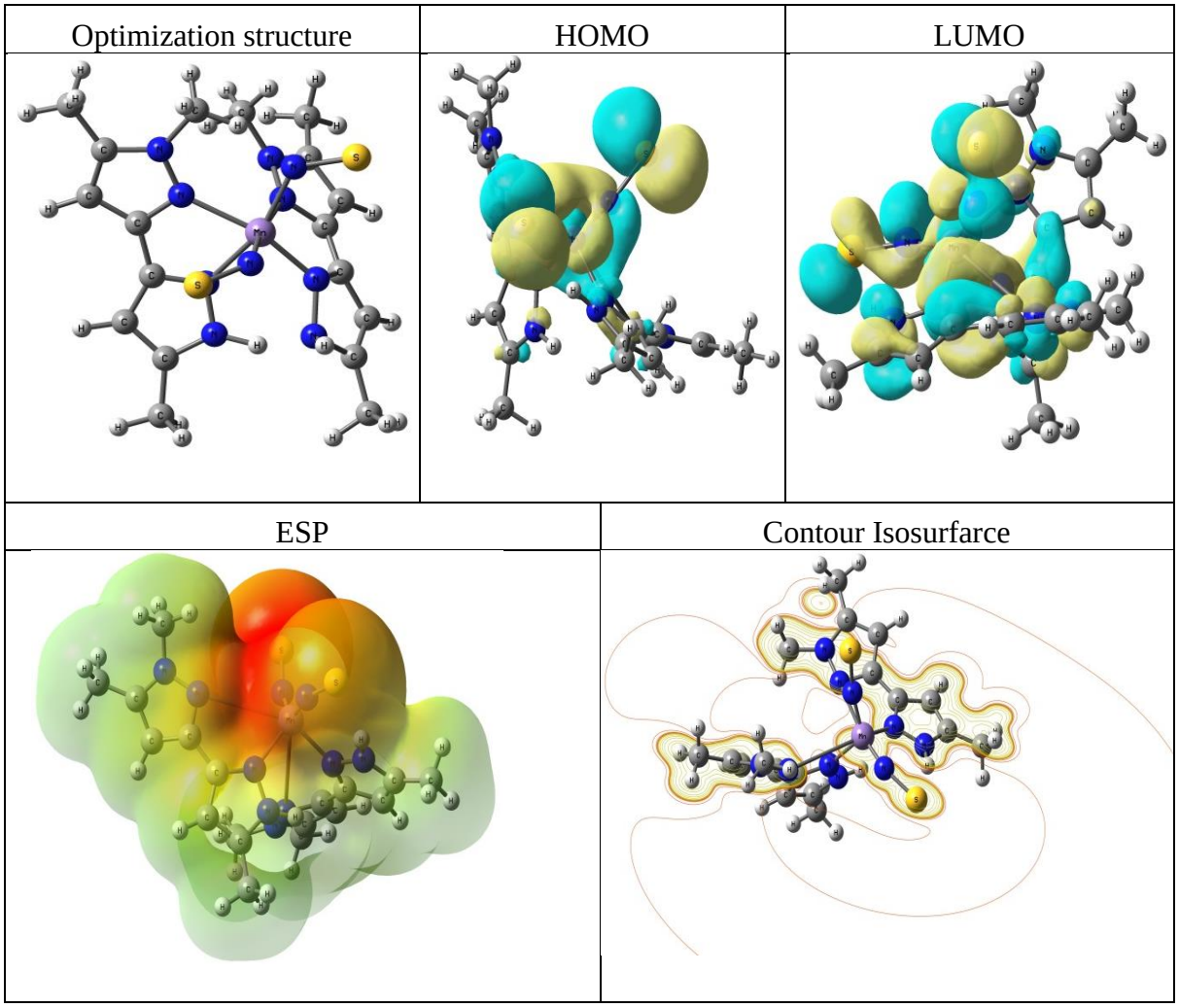

Figure 9. The HOMO, LUMO, optimized structure, electrostatic potential and contour isosurface representation (negative (red) and positive (blue) regions) of C3 inhibitor using DFT/B3LYP method with LANL2DZ basis set

Figure 9 shows the optimized structure, electrostatic potential (ESP) and contour isosurface representation of the C3 molecule studied. We found that the lobes of the orbitals of HOMO

and LUMO are mostly located in the center of the complex and around the sulfur, nitrogen and manganese atoms, which explains that the latter are is ive sites of the reactivity of the C3 inhibitor and at through which it is adsorbed on the surface of the metal [43]. Concerning the analysis of the ESP and Contour representations, the potential and the electronic density increase in the following order: blue<green<yellow<Red [18]. Examination of the ESP and Contour maps showed that the electron-rich regions (red color) are located in the center and around the sulfur atoms. This indicates that this complex reacts with the metal surface through these nucleophilic sites rich in electron density. This suggests the adsorption spontaneity of C3 on the mild steel surface.

3.8. Monte Carlo simulations

To comprehend how well complex C3 inhibits corrosion on the surface of Fe (1 1 0) metal in a 1 M HCl medium, Monte Carlo simulation has been run. 53 water molecules, 3 chloride ions, and 3 hydronium ions make up the system used for the simulation. The visual top and side images of the conformational structure of C3 inhibitor adsorbed on the metal surface are shown in (Figure 10).

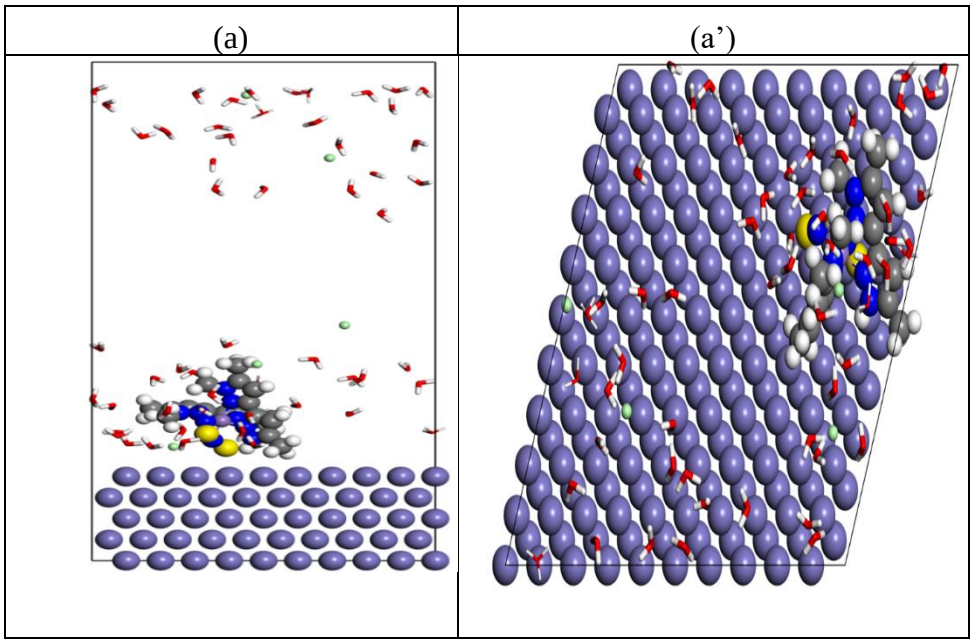

Figure 10. Side (a) and top (a') views of the stable adsorption of Fe (110) /C_3

From this Figure we found that the C3 molecule is placed almost at the metal surface, and it is clear that the C3 compound is adsorbed in a perpendicular manner on the Fe (1 1 0) interface by these functional groups (N=S are attracted to the metal surface). This indicates that the inhibitor forms a protective barrier against the aggressive media, which suggests the increasing inhibition efficiency. According to this method, we calculated the binding and

adsorption energies which take place between the molecule C3 and the metal surface Fe (1 1 0), using the formula below [44,45]:

$$E_{ads} = -E_{bind} = E_{total} - (E_{surface+\ solution} + E_{inhibitor+\ solution}) + E_{solution} \quad (9)$$

where E_{ads} represents the adsorption energy, $E_{\mathbf{total}}$ the total energy of the system (includes the bulk metal as well as the inhibitor molecules adsorbed on the Fer crystal and the acid solution), $E_{surface+\ solution}$ is the total energy of the system without any molecule of inhibitor, $E_{solution}$ denotes the total energy of the solution and $E_{inhibitor+\ solution}$ represents the total energy of the system without the Fe crystal, respectively. The calculated binding and adsorption energies showed that the calculated adsorption energy (-209.851 kJ/mol) is a very negative value, which suggests that the C3 complex is spontaneously adsorbed on the metal surface [4]. This large energy value also shows that the C3 inhibitor is very effective, if compared by other previous work [12,16,21]. The high energy value of E_{bind} indicates a stable and potent interaction of the C3 compound at the mild steel interface [46]. These reinforce the experimental and quantum results obtained.

4. CONCLUSION

In the context of showing the effect of new coordination complexes on corrosion inhibition of mild steel in an acidic medium, we tested the mononuclear manganese (II) coordination complexes which are bound to the metal centers of Mn. The following conclusions were drawn as a result of the varied results:

- The experimental results revealed the strong corrosion inhibition efficiency of this complex.
- Inhibitory efficacy values increased with increasing concentration, reaching 96.3% at a concentration of10^{-3} M.
- SEM images confirmed the formation of a strong bond between NCS and Fe ions to form a stable complex.
- DFT computational indicated that this complex reacts with the metal surface through the nucleophilic sites rich in electron density.
- MC simulation revealed that the C3 complex is spontaneously adsorbed on the metal surface.

Acknowledgments

We thank all colleagues.

Declaration of competing interest

The authors declare no conflict of interests.

REFERENCES

[1] S. Paul, and I. Koley, J. Bio- Tribo-Corrosion 2 (2016).
[2] J.L. Alamilla, M.A. Espinosa-Medina, and E. Sosa, Corros. Sci. 51 (2009) 2628.
[3] K. Tebbji, A. Aouniti, A. Attayibat, B. Hammouti, H. Oudda, M. Benkaddour, S. Radi, and A. Nahle, Indian J. Chem. Technol. 18 (2011) 244.
[4] A. Jmiai, B. El Ibrahimi, A. Tara, R. Oukhrib, S. El Issami, O. Jbara, L. Bazzi, and M. Hilali, Cellulose 24 (2017) 3843.
[5] Y. Hu, Y. Dong, X. Sun, G. Zuo, J. Yin, and S.H. Liu, Pigment 156 (2018) 260.
[6] H. He, L. Hashemi, M.L. Hu, and A. Morsali, Coord. Chem. Rev. 376 (2018) 319.
[7] R. Vilar, Eur. J. Inorg. Chem. 2008 (2008) 357.
[8] A.E. Regazzoni, and M.A. Blesa, Langmuir 7 (1991) 473.
[9] M. Mahdavian, and M.M. Attar, Corros. Sci. 51 (2009) 409.
[10] T.I. Kashar, K.M. Emran, and A. Mo'ala, Arab. J. Chem. Environ. Res. 07 (2020) 29.
[11] L.H. Abdel-Rahman, N.M. Ismail, M. Ismael, A.M. Abu-Dief, and E.A.-H. Ahmed, J. Mol. Struct. 1134 (2017) 851.
[12] A. Radi, B. El Mahi, A. Aouniti, M. El Massoudi, S. Radi, M. Kaddouri, T. Chelfi, A. Jmiai, A. El Asri, B. Hammouti, I. Warad, A. Guenbour, and A. Zarrouk, Chem. Phys. Lett. 795 (2022) 139532.
[13] M. El-Massaoudi, S. Radi, Y.N. Mabkhot, S.S. Al–Showiman, H.A. Ghabbour, M. Ferbinteanu, N.N. Adarsh, and Y. Garcia, Inorganica Chim. Acta 482 (2018) 411.
[14] M. Kaddouri, M. Bouklah, S. Rekkab, R. Touzani, S.S. Al-Deyab, B. Hammouti, A. Aouniti, and Z. Kabouche, Int. J. Electrochem. Sci. 7 (2012) 9004.
[15] M. Kaddouri, S. Rekkab, M. Bouklah, B. Hammouti, A. Aouniti, and Z. Kabouche, Res. Chem. Intermed. 39 (2013) 3649.
[16] M. Rbaa, A.S. Abousalem, M.E. Touhami, I. Warad, F. Bentiss, B. Lakhrissi, and A. Zarrouk, J. Mol. Liq. 290 (2019) 111243.
[17] A. Imjjad, K. Abbiche, M.D. Mellaoui, A. Jmiai, N. El Baraka, A. Ait Taleb, I. Bazzi, S. El Issami, M. Hilali, R. Ben Said, and M. Hochlaf, Appl. Surf. Sci. 576 (2022) 151780.
[18] A. Jmiai, A. Tara, S. El Issami, M. Hilali, O. Jbara, and L. Bazzi, J. Mol. Liq. 322 (2021) 114509.
[19] B. El Ibrahimi, K. El Mouaden, A. Jmiai, A. Baddouh, S. El Issami, L. Bazzi, and M. Hilali, Surfaces and Interfaces 17 (2019) 100343.
[20] I. Annergren, M. Keddam, H. Takenouti, and D. Thierry, Electrochim. Acta 41 (1996) 1121.
[21] M. Rbaa, F. Benhiba, M. Galai, A.S. Abousalem, M. Ouakki, C.H. Lai, B. Lakhrissi, C. Jama, I. Warad, M. Ebn Touhami, and A. Zarrouk, Chem. Phys. Lett. 754 (2020) 137771.
[22] F. Bentiss, M. Bouanis, B. Mernari, M. Traisnel, H. Vezin, and M. Lagrenée, Appl. Surf.

Sci. 253 (2007) 3696.
[23] A.M. Abdel-Gaber, B.A. Abd-El-Nabey, I.M. Sidahmed, A.M. El-Zayady, and M. Saadawy, Corros. Sci. 48 (2006) 2765.
[24] K. Cherrak, M. El Massaoudi, H. Outada, M. Taleb, H. Lgaz, A. Zarrouk, S. Radi, and A. Dafali, J. Mol. Liq. 342 (2021) 117507.
[25] A. Jmiai, B. El Ibrahimi, A. Tara, S. El Issami, O. Jbara, and L. Bazzi, J. Mol. Struct. 1157 (2018) 408.
[26] S.S. Abd El-Rehim, M.A.M. Deyab, H.H. Hassan, and A.A.A. Ibrahim, 230 (2016) 1641.
[27] A. El-Asri, A. Jmiai, Y. Lin, A. Taoufyq, M.M. Rguiti, H. Bourzi, S. El Issami, Corros. Eng. Sci. Technol. 57 (2022) 680.
[28] Y. ELouadi, F. Abrigach, A. Bouyanzer, R. Touzani, O. Riant, B. ElMahi, A. El Assyry, S. Radi, A. Zarrouk, and B. Hammouti, Der Pharma Chem. 7 (2015) 265.
[29] A.M. El Defrawy, M. Abdallah, and J.H. Al-Fahemi, J. Mol. Liq. 288 (2019) 110994.
[30] R. Nabah, F. Benhiba, Y. Ramli, M. Ouakki, M. Cherkaoui, H. Oudda, R. Touir, I. Warad, and A. Zarrouk, Anal. Bioanal. Electrochem. 10 (2018) 1375.
[31] H. Ouici, M. Tourabi, O. Benali, C. Selles, C. Jama, A. Zarrouk, and F. Bentiss, J. Electroanal. Chem. 803 (2017) 125.
[32] H. Zarrok, A. Zarrouk, R. Salghi, H. Oudda, B. Hammouti, M. Ebn Touhami, M. Bouachrine, and O.H. Pucci, Electrochim. Acta 30 (2012) 405.
[33] A. Jmiai, B. El Ibrahimi, A. Tara, M. Chadili, S. El Issami, O. Jbara, A. Khallaayoun, and L. Bazzi, J. Mol. Liq. 268 (2018) 102.
[34] A. Ghazoui, R. Saddik, N. Benchat, B. Hammouti, M. Guenbour, A. Zarrouk, and M. Ramdani, Der Pharma Chem. 4 (2012) 352.
[35] A. Zarrouk, B. Hammouti, S.S. Al-Deyab, R. Salghi, H. Zarrok, C. Jama, and F. Bentiss, Int. J. Electrochem. Sci. 7 (2012) 5997.
[36] A.D. Naik, B. Tinant, K. Muffler, J.A. Wolny, V. Schünemann, and Y. Garcia, J. Solid State Chem. 182 (2009) 1365.
[37] Y. Garcia, V. Ksenofontov, G. Levchenko, G. Schmitt, and P. Gütlich, J. Phys. Chem. B 104 (2000) 5047.
[38] N.A. Wazzan, J. Ind. Eng. Chem. 26 (2015) 291.
[39] I.B. Obot, D.D. Macdonald, and Z.M. Gasem, Corros. Sci. 99 (2015) 1.
[40] M. Yadav, S. Kumar, R.R. Sinha, I. Bahadur, and E.E. Ebenso, J. Mol. Liq. 211 (2015) 135.
[41] S.K. Saha, M. Murmu, N.C. Murmu, and P. Banerjee, J. Mol. Liq. 224 (2016) 629.
[42] V. Saraswat, M. Yadav, and I.B. Obot, Colloids Surfaces A Physicochem. Eng. Asp., 599 (2020) 124881.
[43] S. Sengupta, M. Murmu, S. Mandal, H. Hirani, and P. Banerjee, Colloids Surfaces A Physicochem. Eng. Asp. 617 (2021) 126314.

[44] K.F. Khaled, Corros. Sci. 52 (2010) 3225.
[45] A. Asan, M. Kabasakalogˇlu, M. Işıklan, and Z. Kılıç, Corros. Sci. 47 (2005) 1534.
[46] V. Kalia, P. Kumar, S. Kumar, M. Goyal, P. Pahuja, G. Jhaa, S. Lata, H. Dahiya, S. Kumar, A. Kumari, and C. Verma, J. Mol. Liq. 348 (2022) 118021.